

Melting Relationships in the System Fe—FeO at High Pressures: Implications for the Composition and Formation of the Earth's Core

Takumi Kato and A.E. Ringwood

Research School of Earth Sciences, Australian National University, Canberra, A.C.T. 2601, Australia

Abstract. A reconnaissance investigation has been carried out on melting relationships in the system Fe—FeO at pressures up to 25 GPa and temperatures up to 2200°C using an MA-8 apparatus. Limited studies were also made of the Co—CoO and Ni—NiO systems. In the system Fe—FeO, the rapid exsolution of FeO from liquids during quenching causes some difficulties in interpretation of textures and phase relationships. The Co—CoO and Ni—NiO systems are more tractable experimentally and provide useful analogues to the Fe—FeO system. It was found that the broad field of liquid immiscibility present at ambient pressure in the Co—CoO system had disappeared at 18 GPa, 2200°C and that the system displayed complete miscibility between molten Co and CoO, analogous to the behaviour of the Ni—NiO system at ambient pressure. The phase diagram of the system Fe—FeO at 16 GPa and from 1600–2200°C was constructed from interpretations based on the textures of quenched run products. The solubility of FeO in molten iron is considerably enhanced by high pressures. At 16 GPa, the Fe—FeO eutectic contains about 10–15 mol percent FeO and the eutectic temperature in this iron-rich region of the system occurs at $1700 \pm 25^\circ\text{C}$, some 350°C below the melting point of pure iron at the same pressure. The solubility of FeO in molten Fe increases rapidly as temperature increases from 1700 to 2200°C. A relatively small liquid immiscibility field is present above 1900°C but is believed to be eliminated above 2200°C. This inference is supported by thermodynamic calculations on the positions of key phase boundaries. A single run carried out on an $\text{Fe}_{50}\text{FeO}_{50}$ composition at 25 GPa and 2200°C demonstrated extensive and probably complete miscibility between Fe and FeO liquids under these conditions.

The melting point of iron is decreased considerably by solution of FeO at high pressures; moreover, the melting point gradient (dP/dT) of the Fe—FeO eutectic is much smaller than that of pure iron and is also smaller than that of mantle pyrolite under the P, T conditions studied. These characteristics make it possible for melting of metal phase and segregation of the core to proceed within the Earth under conditions where most of the mantle remains below solidus temperatures. Under these conditions, the core would inevitably contain a large proportion of dissolved FeO. It is concluded therefore, that oxygen is likely to be the principal light element in the core. The inner core may not be composed of pure iron, as often proposed. Instead, it may consist of a crystalline oxide solid solution $(\text{Ni}, \text{Fe})_2\text{O}$.

1. Introduction

It is well known that the density of the outer core is about 10 percent smaller than that of pure iron under corresponding P, T conditions, implying the presence of one or more light elements in this region of the Earth (Birch 1964). Several authors, including Dubrovskiy and Pan'kov (1972) have suggested on rather general grounds that oxygen may be the principal light element in the core. A problem encountered by this hypothesis is the limited solubility of oxygen in molten iron. At the relevant eutectic temperature in the system Fe—FeO, molten iron dissolves only 0.16 weight percent of oxygen and an extensive liquid immiscibility field extends across the system above this temperature (Fig. 1).

Ringwood (1977) extrapolated earlier experimental data on the solubility of oxygen in iron between 1523–1960°C and concluded that Fe and FeO should become extensively miscible at core temperatures ($\approx 3000^\circ\text{C}$). He also predicted that miscibility would be enhanced by high pressures and that wüstite would transform from the ionic to the metallic state at about 30 GPa. In the light of these relationships, he concluded that the core contained about 10 weight percent of oxygen, and that this element was the principal

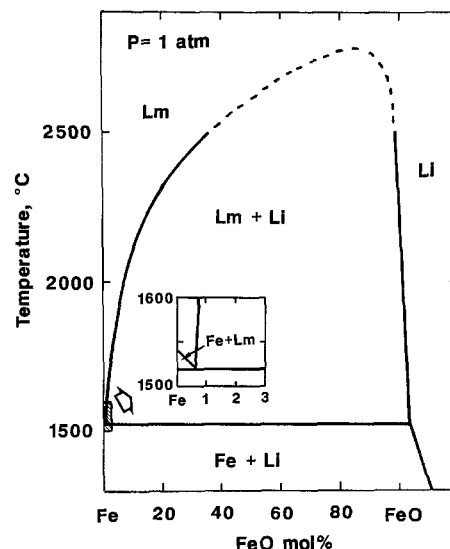


Fig. 1. Phase diagram of the system Fe—FeO at ambient pressure based on the results of Fischer and Schumacher (1977) and Ohtani et al. (1989). Lm, Fe-rich metallic liquid; Li, FeO-rich ionic liquid

light component of the core. Subsequent studies have provided a large measure of confirmation for these predictions. Ohtani and Ringwood (1984) demonstrated experimentally that FeO is extensively soluble in molten Fe at 2500°C and that complete miscibility is probably achieved above 2800°C (Fig. 1). Ohtani et al. (1984) also demonstrated that high pressure considerably enhances the solubility of FeO in Fe and concluded that the miscibility gap in the Fe–FeO system disappears around 20 GPa. Knittle and Jeanloz (1986) demonstrated that FeO transforms to the metallic state at about 70 GPa. Jeanloz and Ahrens (1980) investigated the behaviour of FeO under shock compression and showed that the density of the core could be explained if it contained 8–10 weight percent of dissolved oxygen. A comprehensive review of the topic was presented by Ringwood (1984) whilst the implications of the results for core-formation in the Earth were explored by McCammon et al. (1983).

Despite this encouraging progress, it remains important to understand the detailed nature of high P , T phase equilibria in the system Fe–FeO in order to clarify the process of core-formation within the Earth. We report herein the results of a set of experiments on the system Fe–FeO at pressures up to 25 GPa in the temperature range 1500–2200°C, using an MA-8 multi-anvil high pressure apparatus. Unfortunately, this system is difficult to investigate by the normal direct techniques because of extremely rapid exsolution of FeO from molten Fe during quenching. This causes ambiguities concerning high pressure equilibria, particularly the extent of the liquid immiscibility field. Consequently, we regard the present study as being in the nature of a reconnaissance investigation. Nevertheless, it has served to establish certain key features of the topology of the system. Parallel investigations on the system Fe–FeO and the related systems Fe–FeO–FeS and Fe–Ni–FeO–FeS also carried out in an MA-8 apparatus have recently been described by M. Kato (1985) and by Urakawa et al. (1987).

Reconnaissance investigations of melting relationships in the systems Ni–NiO, Co–CoO and Co–CoO–MgO at 3 GPa were carried out by Ringwood and Major (1982) and Ohtani et al. (1984). These systems are analogous in some respects to the system Fe–FeO. However, they are more tractable experimentally because of the high melting points of the oxides as compared to FeO and the lower diffusion rates of oxygen in the molten alloys, which permit the textures resulting from high temperature equilibria to be retained during quenching. The behaviour of these systems can therefore provide additional insight into phase equilibria in the system Fe–FeO. Accordingly, we have also carried out a few additional experiments the systems Co–CoO and Ni–NiO in pursuit of this objective.

2. Experimental Methods

Most of the high pressure experiments were carried out in an MA-8 apparatus using tungsten carbide cubes possessing truncation edge lengths of 3.5 mm. The apparatus and pressure calibrations at room temperature and at high temperature have been described by Ohtani et al. (1986). Most of the present experiments were carried out at 16 GPa. However one key experiment was carried out at 25 GPa using anvils with 2.0 mm truncations. Estimated uncertain-

ties in pressures at run temperatures are about 5 percent of the nominal values.

The furnace assembly used was essentially the same as that described by Kato and Kumazawa (1986). The heater consists of two electrically conducting strips fabricated from a mixture of tungsten carbide and diamond powders. The temperature distribution within this heater has been investigated by Irihara and Hibberd (1985) and was shown to be much more uniform than in a cylindrical heater. The pressure medium consisted of an octahedron of sintered magnesium oxide-cobalt oxide solid solution ($Mg_{0.9}Co_{0.1}O$, possessing 30 percent of residual porosity which was calcined at 1000°C for 10 h prior to use. Starting materials consisted of intimate mixtures of high-purity metallic iron and ferric oxide powders (which react promptly to form the desired $Fe + FeO$ assemblage at temperatures of 700–800°C during the heating cycle). The mixtures were placed in tubes of pure MgO (0.6 mm ID, 1.0 mm OD) which were inserted in holes drilled into the pressure medium between the heaters. A few runs were also carried out on mixtures of pure metallic cobalt and cobalt oxide powders. In these systems, equilibrium is believed to be attained very rapidly, within a few seconds, and run-times were therefore short, typically 1–2 min. Reaction of iron and cobalt oxides with the magnesium oxide containers is minimal under these conditions, as shown by electroprobe microanalyses described subsequently.

In order to facilitate interpretation of results, it was found desirable to run two charges possessing differing compositions simultaneously under identical P , T conditions. The experimental arrangement is shown in Figure 2. The MgO tubes containing the samples are located in parallel between the sheet heaters. The distance between the heater and the central region of the samples is about 1 mm and the centres of the samples are 1.5 mm apart. The temperature calibration of this cell (Irihara and Hibberd 1985) showed that the temperatures of the sample cores in both positions were essentially identical (within 20°C).

This configuration has the disadvantage that it is not possible to introduce a thermocouple into the hotspot between the samples without encountering serious contamination. Accordingly the temperature of the hotspot was obtained from a calibration curve of power input versus temperature as determined by a $W_{97}Re_3 - W_{75}Re_{25}$ thermocouple placed in the hotspot in the absence of a metallic sample. The calibration curve has been well established from about 100 previous runs using this furnace assembly and the reproducibility of hotspot temperature is considered to be about $\pm 25^\circ C$. No correction has been applied for the possible effect of pressure on thermocouple EMF, so that a significant additional uncertainty in absolute temperature, as much as 100°C (Getting et al. 1965; Kato and Kumazawa 1986) may be present. However, errors from this source are systematic, so that relative temperatures which are important in establishing the topology of the Fe–FeO phase diagram (at 16 GPa) are unaffected. In addition to the approach described above, three runs were carried out in which a thermocouple was inserted into one of the two MgO tubes. The temperatures thereby measured agreed closely ($< 25^\circ C$) with those derived from the empirical power versus temperature relationship.

After completion of runs, samples were quenched by terminating the power, causing the temperature of the sample to fall below 200°C in a few seconds. Pressure was

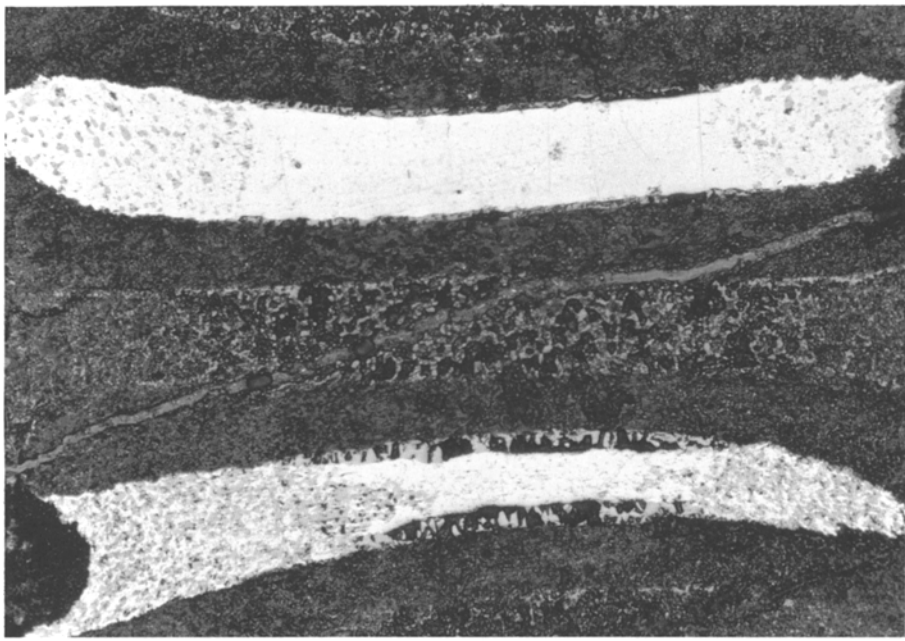


Fig. 2. Cross-section of Run 13 showing the sample assemblies used in the present experiments. Two samples 13-20 and 13-50 were run at the same pressure (16 GPa) and temperature (1900° C) in capsules consisting of fine MgO tubes. Melting occurred in the hotspots in the central regions whereas the extremities of the charges remained unmelted. Note the extensive unmixing of FeO and its migration to form discrete FeO layers (gray) at the top and bottom of the samples, which occurred during the run. The FeO layers in sample 13-50 are about 300 microns wide. The central pool of metal contains numerous dendrites of FeO which crystallized during quenching. The darker regions outside the FeO zones are the MgO capsules. This run illustrates the rapid unmixing of FeO and Fe which occurs in runs carried out near or within the liquid immiscibility field

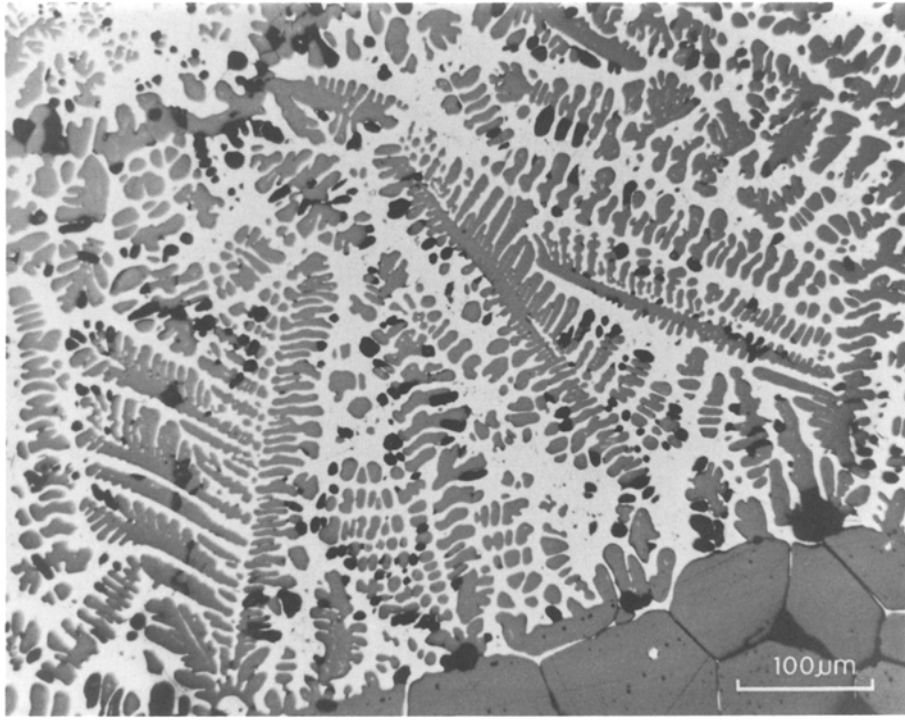


Fig. 3. Texture showing complete liquid miscibility in the system of Ni–NiO at 3 GPa and 1800° C, from Ringwood and Major (1982). Dendritic crystals of NiO (dark in reflected light) in Ni matrix (bright) are formed during quenching from a homogeneous liquid

then released. Samples were polished and studied by reflection microscopy and electronprobe microanalysis.

3. The Systems Ni–NiO and Co–CoO

Ringwood and Major (1982) found that Ni and NiO were completely miscible in the molten state at 3 GPa and formed a simple eutectic system. During quenching, crystalline NiO dendrites precipitated from the Ni–NiO liquid as shown in Figure 3. The similarity to FeO dendrites formed in later runs during quenching of Fe–FeO liquids below 1900° C at 16 GPa is notable (Fig. 6c).

Phase relations in the system Co–CoO are closely analogous to those of Fe–FeO. The solubility of CoO in molten cobalt is similar to that of FeO in molten Fe (Tankens et al. 1964) as shown in Figure 4a. Ohtani et al. (1984) showed that at 3 GPa, the solubility of CoO in molten Co increased rapidly with temperature above 2200° C and that complete miscibility would be achieved above about 3000° C (Fig. 4b).

A sample of molten cobalt saturated with cobalt oxide quenched from 2200° C at 3 GPa is shown in Figure 5a. The cobalt oxide has precipitated in the form of numerous dragonfly dendrites – c.f. FeO dendrites in Figure 6c. The

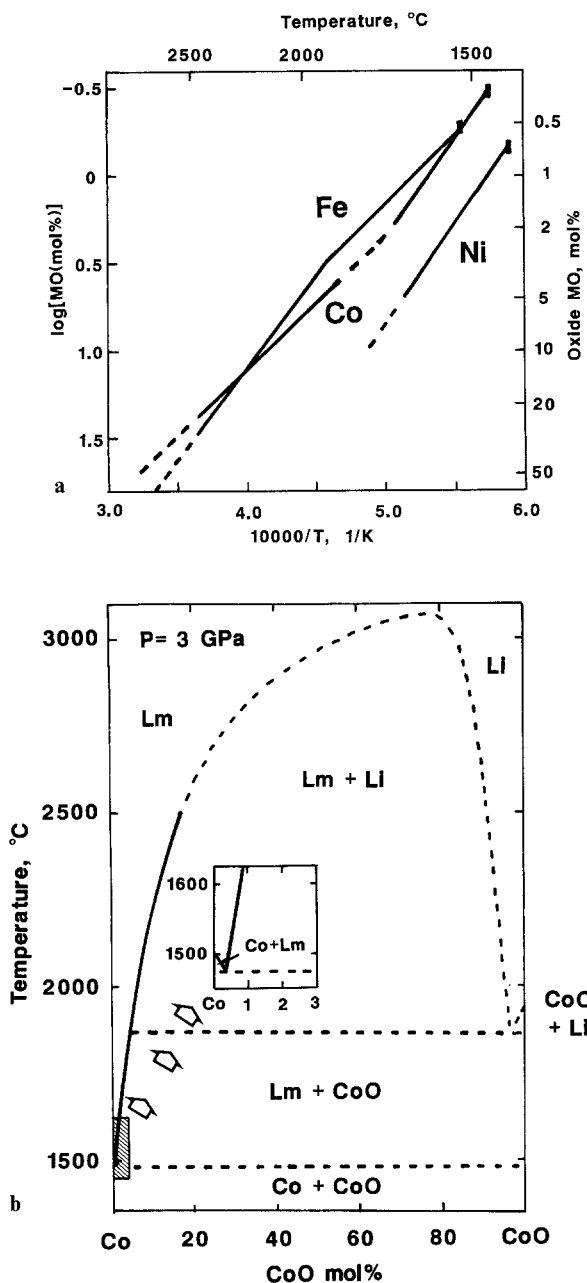


Fig. 4a, b. Solubility of oxygen in molten iron, cobalt and nickel. (a) Solubility data for Fe, Co and Ni at low pressures ($< 3 \text{ GPa}$). The vertical dash on the right end of each line shows the melting temperature. Fe–O solubility after Fischer and Schumacher (1977) between 1520° and 2050° C at ambient pressure and Ohtani and Ringwood (1984) between 2100° and 2550° C at 2 GPa . Co–O solubility after Tankens et al. (1958) between 1560° and 1700° C at ambient pressure and Ohtani et al. (1984) between 1900° and 2500° C at 3 GPa . Ni–O solubility after Tankens et al. (1958) between 1460° and 1700° C at ambient pressure. The difference between Co–O and Fe–O solubilities is quite small in the temperature range of these investigations. (b) Phase diagram of the system Co–CoO at 3 GPa after Ohtani et al. (1984). (Lm, Co-rich metallic liquid; Li, CoO-rich ionic liquid)

solubility of CoO in molten cobalt under these conditions is estimated as about 5–10 percent. A second run was carried out at 2200° C and 18 GPa on a mixture of Co (50%) and CoO (50%). The results are shown in Figure 5b. The quenched melt has a very similar texture to the Ni–NiO

sample (Fig. 3). It demonstrates essentially complete miscibility in the liquid state between Co and CoO under these conditions. In contrast, at low pressures at 2200° C , the system Co–CoO displays a broad field of liquid immiscibility, qualitatively similar to the corresponding field of immiscibility in the system Fe–FeO (Figs. 1, 4b). The above experiments on the system Co–CoO thus demonstrate the dramatic increase in the solubility of CoO in molten cobalt caused by high pressure. We demonstrate below that the system Fe–FeO displays closely analogous behaviour at high pressures.

4. The System Fe–FeO at 16 GPa

Following the terminology of Ringwood (1977) and as shown in Figure 1, we designate metallic liquids comprised predominantly of iron with interstitial oxygen in solution as Lm, and predominantly ionic FeO-rich liquids as Li. Liquid and crystalline FeO are denoted as FeO_l and FeO_c ; likewise for liquid and crystalline iron (Fe_l and Fe_c).

The conditions and results of the experiments are summarised in Table 1. Phase assemblages in the system Fe–FeO were interpreted mainly from microscopic observations of the textures displayed by quenched samples in reflected light. Some aspects of these interpretations are ambiguous because of extremely rapid diffusion of oxygen through iron during the quenching process, as described by Ohtani and Ringwood (1984). This may cause unmixing of iron (Lm) and iron oxide (Li) liquid solutions during quenching. Moreover, crystalline FeO may exsolve from Fe–O liquid (Lm) solutions and migrate to the margin of the charge during quenching. Accordingly, it is not possible to delineate the boundaries of the (Lm + Li) liquid immiscibility field by the quenching method. It is also difficult to determine liquidus temperatures in FeO-rich compositions.

Because of exsolution of oxygen (as FeO) during quenching, estimation of the equilibrium oxygen contents of metallic iron-oxygen solutions by electron microprobe analysis of quenched samples is generally unreliable and usually leads to serious underestimates (e.g. M. Kato 1985), as described later in this paper.

On the other hand, careful study of microtextures displayed by samples with variable starting compositions can identify the temperature of the Fe_c – FeO_c eutectic and the position of the Fe_c – FeO_c eutectic composition. Moreover, the depression of the melting point of iron by solution of FeO can readily be measured because of drastic textural differences above and below the eutectic temperature. This has a strong influence on the topology of the Fe–FeO phase diagram and provides an independent check upon the position of the Fe_c – FeO_c eutectic as shown in Section 5. The usual morphological criteria for identifying primary crystals, the onset of melting, and quenched liquids (Lm and Li) are also applicable.

Intermediate compositions ($\text{FeO}: 20$ and $50 \text{ mol } \%$)

In subsequent descriptions, samples are denoted by two numbers (e.g. 16-20) the first of which denotes the run number as given in Table 1 and the second denotes the molecular percentage of FeO in the bulk composition.

Samples 16-20 at 1600° C consist of two irregular polyhedral domains with representative scales of 50 microns

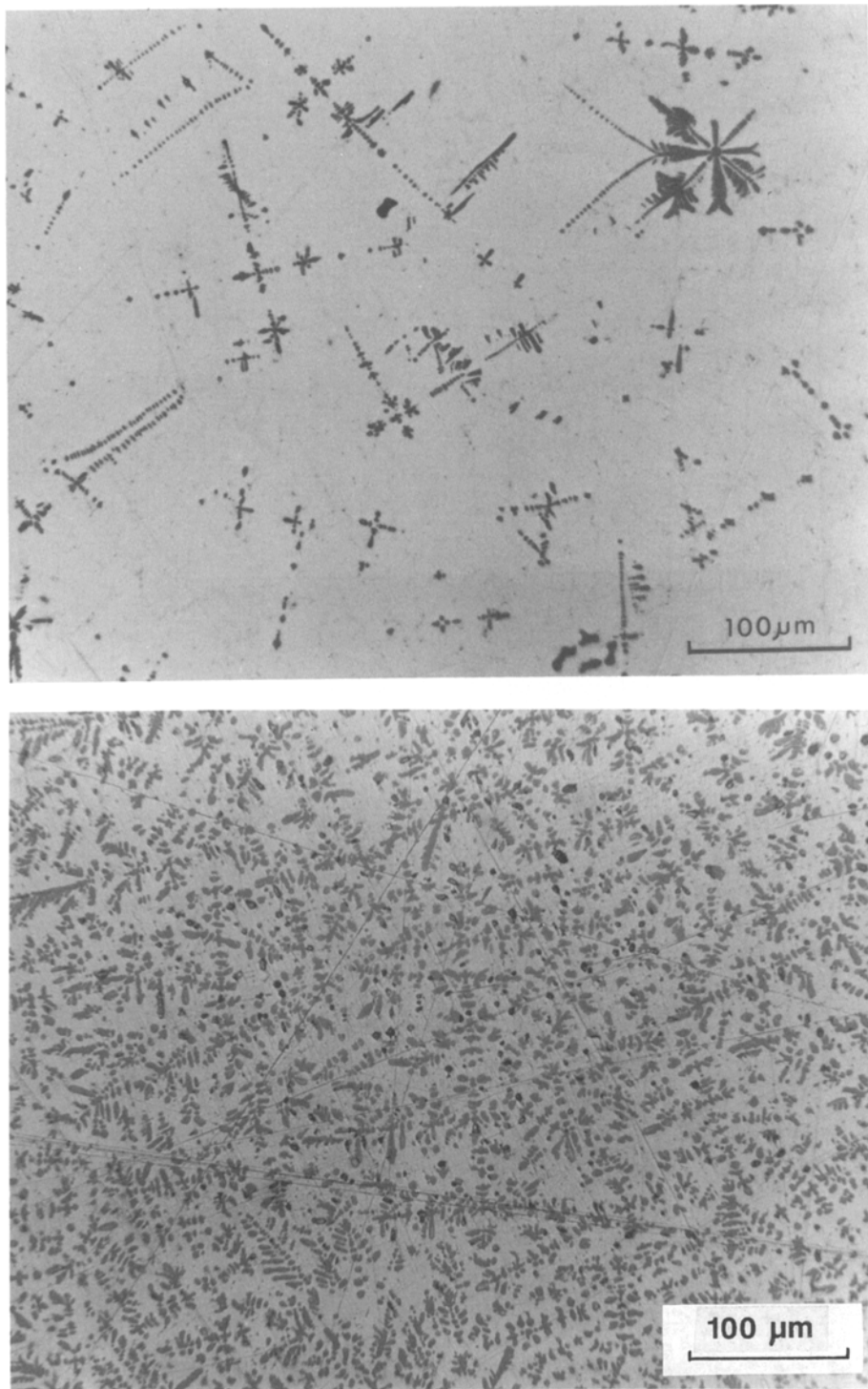


Fig. 5a, b. Textures displayed by quenched products in the system Co–CoO in reflected light. Dark regions represent CoO crystals, whilst bright regions represent Co metal. (a) At 18 GPa and 2200° C, small amounts of CoO (5–10%) dissolved in the metallic liquid are exsolved during quenching and crystallized as dendrites (from Ringwood and Major 1982). (b) At 18 GPa and 2200° C, abundant CoO dendrites similar to those in the system Ni–NiO (Fig. 3) are observed. The figure displays a large increase in solubility of CoO in Co caused by the high pressure and indicates complete miscibility between molten CoO and Co under the run conditions

(Fig. 6a), one of which is composed of metallic iron and the other of FeO containing small inclusions (~5 microns) of metallic Fe. Finely dispersed FeO grains are observed at the boundaries between the domains. This texture indicates recrystallisation and growth of Fe and FeO under subsolidus conditions by oxygen diffusion. The stable phase assemblage is $\text{Fe}_c + \text{FeO}_c$.

The texture of sample 4-50 at 1700° C is dramatically different. Metallic iron has segregated into the core of the tube and is surrounded by FeO crystals (Fig. 6b). This central metallic region contains two types of exsolved FeO

inclusions: (i) dragonfly-shaped dendrites with dimensions 10–100 microns, (ii) fine spheroidal submicron particles, uniformly distributed. The gross segregation of metal from oxide combined with the crystallization of FeO dendrites within the metal show clearly that the metal was originally molten and contained a significant amount of oxygen in solution. A similar texture is displayed by samples 22-20 at 1700° C and 7-50 at 1800° C (Fig. 6c). The stable phase assemblage in these samples under the run conditions is ($\text{Lm} + \text{FeO}_c$).

Sample 13-50 at 1900° C displays the same assemblage

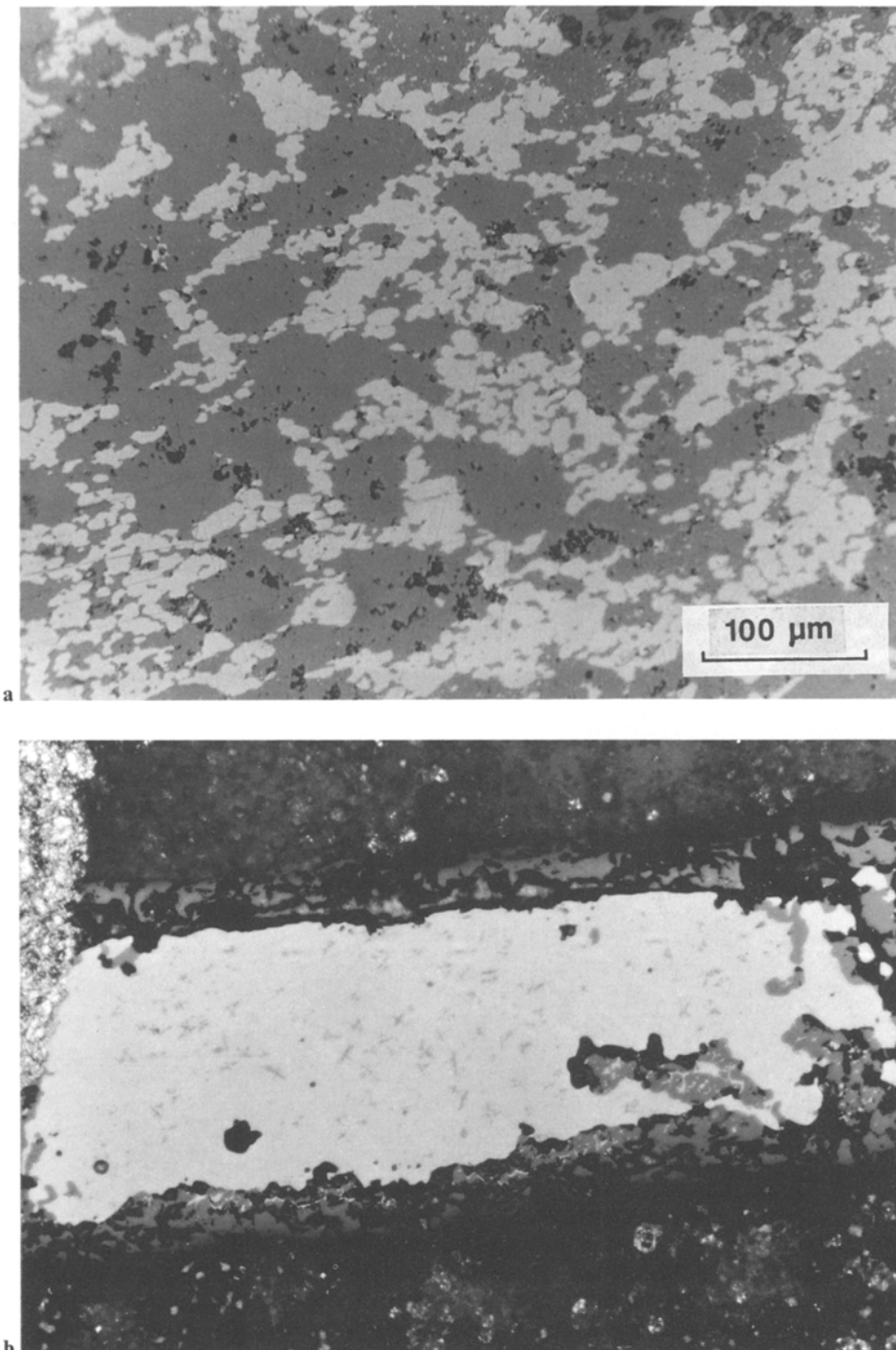
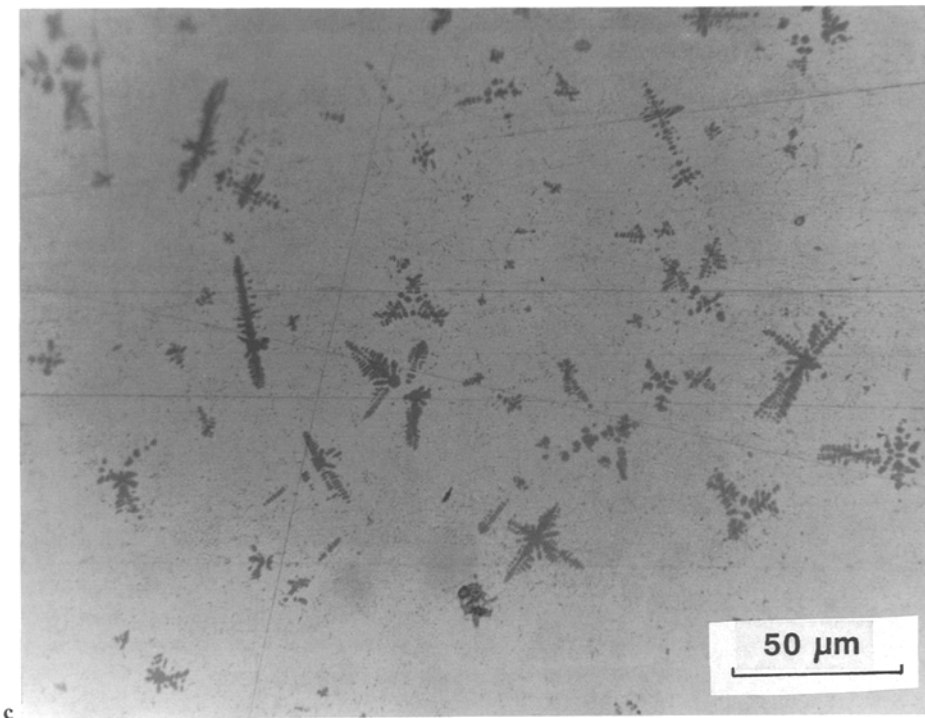


Fig. 6a-e. Photomicrographs of run products in the system Fe—FeO at 16 GPa. Dark regions represent FeO crystals in reflected light, whilst bright regions represent Fe metal. (a) Sample 16-50 at 1600° C, showing an assemblage of Fe + FeO_c just below the solidus. (b) Sample 4-50 at 1700° C. Melting has occurred within Lm + FeO field leading to extensive segregation of FeO at the top and bottom of the metallic core. The latter contains numerous dendrites of crystalline FeO formed during quenching. Note the contrast in textures between this run, conducted just above the solidus, and sample 16-50 (Fig. 6a) which remained below the solidus. (c) Sample 7-50 at 1800° C, showing FeO dendrites formed from the metallic liquid during quenching. Excess FeO not dissolved in Fe has segregated to the margin of the sample during the run. (d) Run 3-50 at 1950° C showing liquid immiscibility characterized by droplets of FeO in an Fe matrix. This run could be interpreted as evidence of liquid immiscibility at the run temperature. Alternatively, the texture may have formed during quenching, when a homogeneous liquid Fe—O solution at 1950° C passed transiently through a small two-liquid field below 1950° C during quenching. The second interpretation is preferred since observations of numerous runs carried out in the primary field of Fe—FeO liquid immiscibility at lower pressure show that essentially complete phase separation and migration of FeO to the margins of the sample occur within a few seconds. Note the contrast, also, with textures in Figures 2 and 6b that display the essentially complete unmixing of Fe and FeO which occurs when runs are carried out above the solidus. (e) Near-eutectic run 21-10 at 1750° C showing primary Fe crystals (light) and interstitial Fe—O quench liquid (cloudy). The texture indicates that the bulk composition containing 10 mole percent FeO lies within the primary crystallization field of Fe

of (Lm + FeO_c). However sample 13-20, obtained simultaneously at 1900° C, also displays small amounts of spherical FeO droplets (10–50 microns) which themselves contain small Fe grains. The compound droplets are distributed throughout a matrix consisting of Fe metal and FeO dendrites. The droplets are identified as quenched FeO-rich ionic liquid (Li) which is immiscible with the metallic liquid under the run conditions. Similar quenched FeO-rich ionic liquids are observed in samples at higher temperatures: 3-50 at 1950° C, 1-20 at 2000° C, 17-50 at 2050° C, 15-20 and 15-50 at 2200° C. The number of immiscible droplets increases dramatically in these samples (Fig. 6d, 3-50) as compared to those in sample 13-20 at 1900° C. These results

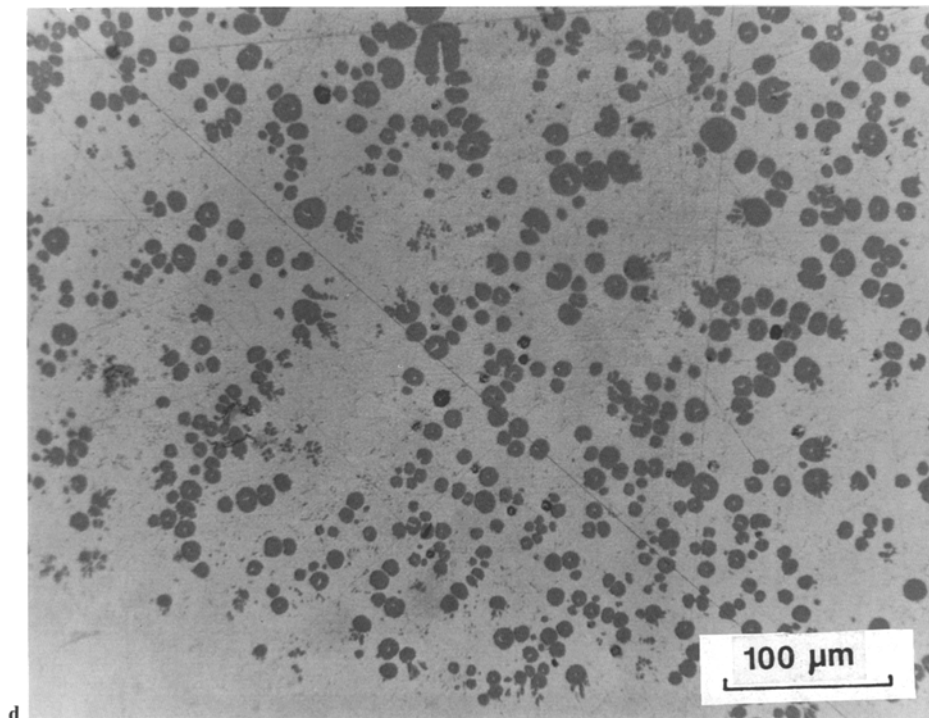
show that the boundary between (Lm + FeO_c) field and the (Lm + Li) liquid immiscibility field must lie very close to 1900° C. This boundary is straddled by runs 13-50 (Lm + FeO_c) and 13-20 (Lm + Li) at 1900° C. The different phase assemblages in the two runs probably arose from the presence of a small temperature gradient across the samples. The eutectic temperature between FeO_c and the ionic (FeO—Fe) liquid is thus placed at 1900° C (Fig. 7).

Because of the rapidity of exsolution from a homogeneous liquid into (Lm + Li) during quenching, it is not possible to establish the upper boundary of the liquid immiscibility field by the quenching method. The broken line shown in Figure 7 is based on calculations as described in Sec-



c

Fig. 6c-d.



d

tion 5. Two runs carried out above this boundary (15-20 and 15-50) at 2200° C showed abundant droplets of Li in a matrix of Lm, similar to the texture shown in Figure 6d. However, this texture could be either an equilibrium or a quenching phenomenon. The droplet texture can be produced when a homogeneous liquid solution cools into the two-liquid field during quenching. The actual liquid immiscibility field may in fact be considerably smaller than the theoretical field indicated in Figure 7 (as discussed further in the caption to Fig. 6d).

FeO-rich composition: FeO: 90 mole percent

In sample 17-90 produced at 2050° C, the central region of the charge consists of a granular mixture of Fe and FeO, whereas the peripheral regions consist solely of FeO. The central granular region is considered to represent a quenched product from the ionic (FeO-Fe) liquid (Li). This is supported by the presence of Li droplets in sample 17-50 which was run at the same time. There are two possible interpretations of the stable phase assemblage repre-

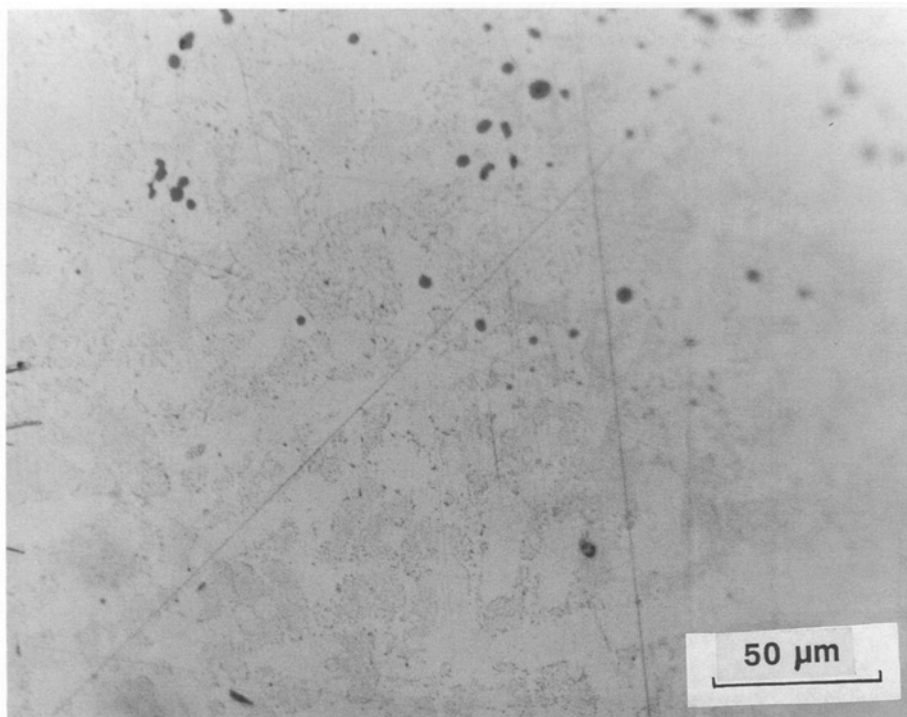


Fig. 6e.

Table 1. Results of melting experiments on the Fe–FeO system at 16 GPa

Run number	Temperature (°C)	Sample 1		Sample 2	
		Composition mol% FeO	Result	Composition mol% FeO	Result
16	1600	20	Fe + FeO	50	Fe + FeO
19	1700	5	Fe + FeO + Lm	10	Fe + FeO + Lm
4	1700	50	FeO + Lm	—	
22	1700	20	FeO + Lm	(thermocouple)	
21	1750	10	Lm(+ Fe)	15	Lm(+ FeO)
7	1800	50	FeO + Lm	(thermocouple)	
13	1900	20	Lm + FeO + Li	50	Lm + FeO
3	1950	50	Lm + Li	—	
1	2000	20	Lm + Li	(thermocouple)	
17	2050	50	Lm + Li	90	Li(+ FeO)
15	2200	20	Lm + Li	50	Lm + Li

Abbreviations: Lm: metallic liquid, Fe-rich liquid solution of Fe–FeO; Li: ionic liquid, FeO-rich liquid solution of Fe–FeO

sented by this texture: (i) FeO grains around the periphery of the charge are primary crystals which crystallized from the melt, i.e., the stable phase assemblage is (FeO_c+Li) or (ii) the peripheral FeO crystals were themselves formed during quenching from a totally liquid state. Whichever interpretation is correct, the eutectic composition between FeO_c and FeO–Fe (Li) would possess a smaller FeO content than the bulk composition of the sample (90 mol %), as indicated in Figure 7.

Fe-rich compositions FeO: 5, 10 and 15 mole percent

Samples 19-5 and 19-10 at 1700° C display mainly subsolidus textures which are similar to those observed in samples 16-20 and 16-50. However the presence of a small amount of liquid in samples 19-5 and 19-10 indicated by the hetero-

geneous distribution of polyhedral FeO grains which are not present in the outer 50 micron rim of the charge and have become concentrated towards the centers of the samples. The combined results from runs 19-5, 19-10, 4-50 and 22-20 indicate that the actual temperature range in these runs (nominally 1700° C) overlaps the Fe–FeO eutectic temperature. The eutectic temperature is thus placed at 1700±25° C.

Samples 21-10 and 21-15 at 1750° C have clearly melted and display an intergrowth of primary metallic iron crystals with regions consisting of an intimate mixture of Fe and submicron FeO grains. The presence of a very small amount of FeO dendrites in 20-15 indicates that the liquid was slightly oversaturated in FeO_c as compared to the eutectic composition. On the other hand, in 22-10 the presence of well-developed (> 50 micron) primary metallic Fe crystals

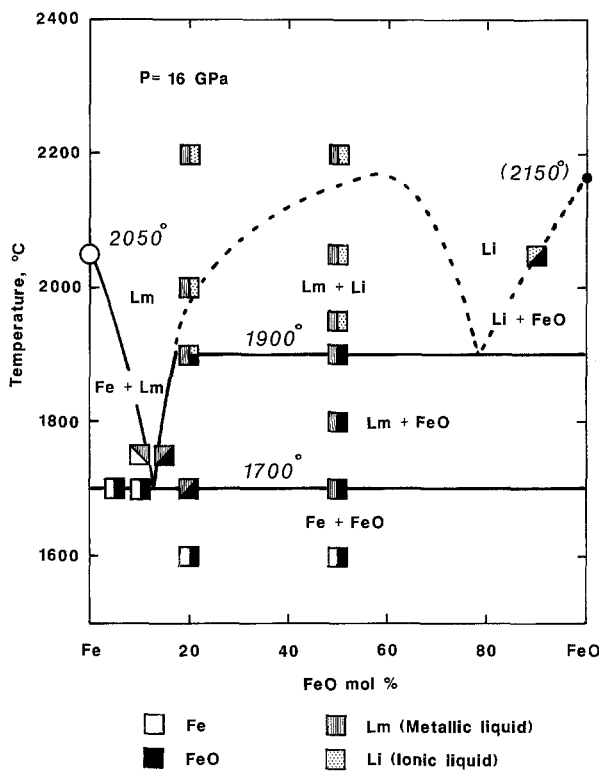


Fig. 7. Phase diagram of the system Fe-FeO at 16 GPa based on the present experimental results. The data points used to construct the diagram are also shown. The melting temperature of FeO is estimated to be 2150°C, based upon an extrapolation of results obtained by Lindsley (1966) and also upon the observation that the melting temperature of FeO is higher than that of Fe by approximately 100°C in this pressure range (Knittle and Jeanloz 1986)

distributed through a matrix extremely fine Fe-FeO quench is considered to represent evidence of oversaturation by metallic iron in the liquid (Fig. 6e) either at run temperature, or during quenching. Because of the quench-crystallization problem, we cannot determine from the textures whether or not the run temperatures exceeded the liquidus of (Fe + Lm) or (FeO + Lm). However, the observations described above indicate that the Fe-FeO eutectic composition is located between the bulk compositions of these samples, i.e. between 10 and 15 mole percent FeO. This is supported by electron-probe analyses for oxygen and thermodynamic calculations discussed subsequently.

Melting Temperature of Pure Iron

The melting temperature of pure iron was also investigated in order to provide a check on the accuracy of temperature measurement in our pressure cell and to provide direct comparisons of the temperature differences between the melting point of pure iron and the two eutectics (Fe-rich and FeO-rich) in the system as shown in Figure 7. The melting point was determined by monitoring the resistance of a length of spec-pure Fe wire inserted in an Al_2O_3 tube (0.6 mm I.D.) as temperature was increased. The melting point was readily identified by a rapid drop in resistance followed by a gradual increase. The melting point of iron was thereby determined to be 1980°C at 12 GPa and 2050°C at 16 GPa. The uncertainties in these temperatures are estimated to be about $\pm 50^\circ\text{C}$ and are caused by two factors: (i) temper-

ature is obtained from the temperature versus power calibration which itself has an uncertainty of $\pm 25^\circ\text{C}$, (ii) the melting signal of iron is spread out over a temperature interval of 25°C . Our results are consistent with those of previous investigations on the melting of iron by Sterrett et al. (1965), who used Pt-Rh thermocouples and by Liu and Bassett (1975) and Boehler (1986) who used optical pyrometry, when reasonable estimates of combined experimental errors arising from the different techniques are considered.

Electron Microprobe Results

It is essential to demonstrate that melting temperatures and phase boundaries in the present experiments have not been influenced by contamination by components of the pressure cell during the experiments. Possible contaminants are carbon and tungsten from the heaters, titanium from the electrodes and magnesium and cobalt from the pressure medium. Accordingly, detailed electron probe analyses of these elements were carried out in a key subset for runs (16-20 and 16-50 at 1600°C, 19-5, 19-10 and 4-50 at 1700°C, 21-10 and 21-15 at 1750°C, 7-50 at 1800°C, 17-50 and 17-90 at 2050°C, 15-20 and 15-50 at 2200°C and also on the sample used in determining the melting point of pure iron at 16 GPa.

The concentrations of W and Ti were below detection limits ($\text{W} \sim 50 \text{ ppm}$, $\text{Ti} \sim 50 \text{ ppm}$) in the above samples. The limits of detection for carbon in the analyses were typically 400–500 ppm at the operating conditions of 15 KV acceleration voltage and a 30 nA current. Concentrations of carbon throughout samples 16-20, 16-50, 19-5, 19-10 and 4-50 were below detection limits. Small amounts of carbon (550–650 ppm) were found in metal near the rims of samples 15-20 and 15-50 but the cores of these samples were below detection limits. Sample 7-50 contained 550–600 ppm C whilst samples 21-10 and 21-15 contained 700–750 ppm C. The maximum carbon concentration observed (750 ppm) would alter the melting temperature in the system Fe-C by less than 10°C (Hansen and Anderko 1958). It is clear that the present results have not been affected significantly by carbon contamination.

Magnesium and cobalt were not detected in either metal or oxide phases within samples run at temperatures up to 1900°C (detection limits for Co and Mg are $\sim 100 \text{ ppm}$). At higher temperatures, a continuous solid solution between FeO and MgO is observed in a boundary layer about 200 microns thick between the charge and the MgO capsule. However, magnesium and cobalt concentrations in FeO dendrites and spherules, and in the metal phase within the interior of these runs are below detection limits.

Electronprobe analyses for oxygen (detection limit 300 ppm) were also made on the homogeneous metallic regions in the same samples that were analysed for carbon. A wide range of oxygen contents between < 0.03 and 2.4 percent was observed. The metallic regions in most samples contained between 0.2 and 0.6 percent oxygen. Lower values were found in regions containing densely-packed dendrites and FeO droplets. Higher values of 1.6–1.8 percent O were found in larger pools of iron, relatively free of FeO crystals, within the interiors of 4-50 and 7-50. It appears that exsolution of oxygen as FeO has been most effective in regions where pre-existing FeO nuclei were abundant. The oxygen found within optically homogeneous

metallic regions may be present in solid solution or as submicroscopic exsolved FeO inclusions.

In most runs, because of rapid exsolution of FeO during quenching, the residual oxygen contents of metallic phases are of little relevance to the equilibrium phase diagram (Fig. 7). However, it is possible that the 1.8 percent oxygen occurring within the metal phase of subsolidus run 4-50 may represent an equilibrium solubility. Useful results were also obtained in run 21-10. This consisted of an assemblage of clear Fe crystals up to 50 microns across with interstitial metallic regions possessing a cloudy appearance (Fig. 6e). Oxygen analyses in regions free of optically resolvable FeO were bimodal. Most regions contained < 300 ppm O whereas other regions contained substantial amounts of oxygen, ranging up to 2.4 percent. The former values probably represent the clear Fe crystals whereas the latter high values were probably obtained on the cloudy interstitial material which is believed to consist of a submicroscopic intergrowth of Fe and FeO together with tiny resolvable crystals of Fe metal. This sample was previously interpreted on textural grounds as a near-eutectic run, with large primary Fe crystals and interstitial Fe–FeO quench liquid in which the Fe crystals grew. The eutectic composition must therefore contain more FeO than is present in the bulk composition (10 mol % FeO). Because of beam overlap on metallic iron crystals, the highest value of 2.4 percent oxygen, equivalent to 8.5 mole percent FeO, provides a minimum value for the actual composition of the interstitial quench Fe–FeO liquid. Also, because this run was carried out above the eutectic, its FeO content would be significantly smaller than the FeO content at the eutectic composition. This was previously estimated from textural observations to be 10-15 mole percent FeO. Thermodynamic calculations in section 5 yield a value of 15 ± 3 mole percent FeO for the eutectic composition. The agreement between the three sources of evidence on the eutectic composition is very satisfactory.

Summary of Results

A phase diagram for the system Fe–FeO at 16 GPa has been constructed on the basis of the experiments and observations previously described and is shown in Figure 7. The melting point of pure FeO has been estimated by an extrapolation (MacCammon et al. 1983) of the experimental data of Lindsley (1966). Although some of the phase boundaries (indicated by broken lines) possess large uncertainties, the following characteristics are believed to be reasonably well established within the limitations previously discussed. Note that the temperatures quoted do not include corrections for the effect of pressure on thermocouple EMFs.

1. The melting temperature of pure iron at 16 GPa is $2050 \pm 50^\circ\text{C}$.
2. The Fe_c –FeO_c eutectic temperature in the iron-rich region of the system occurs at $1700 \pm 25^\circ\text{C}$.
3. The composition of this eutectic is located between FeO contents of 10 and 15 mole percent.
4. The FeO_c–Li eutectic temperature in the FeO-rich region of the system occurs at $1900 \pm 25^\circ\text{C}$.
5. The position of this latter eutectic is located at a composition less than 90 mole percent FeO.
6. A field of liquid immiscibility is present above 1900°C but could be much smaller than the theoretically calculated field in Figure 7.

5. Thermodynamic Relationships in the Fe–FeO System at 16 GPa

In this section, thermodynamic calculations of phase relationships are carried out in order to check their consistency with interpretations based on textural observations. We consider firstly the position of the Fe–FeO eutectic in metal-rich compositions. The key experimental observation necessary for this calculation is that solution of FeO in iron causes its melting point to be depressed by 350°C (ΔT^m) at the eutectic composition (Fig. 7). This figure is based upon the results of several runs on different compositions. Systematic errors such as the effect of pressure on thermocouple EMF and characteristics of the pressure cell cancel each other to a considerable degree and we estimate that the error in ΔT^m is about $\pm 75^\circ\text{C}$.

The position of the liquidus phase boundary between (Fe + Lm) and Lm (Fig. 7) at temperature T can be calculated from the Van't Hoff equation for the depression of the melting point of a solid (Fe) by a solute (FeO). This equation can be reformulated as follows (Wood and Fraser 1977).

$$\ln \alpha_{\text{Fe}} = \Delta S_{\text{Fe}}/R (1 - T_{\text{Fe}}^m/T)$$

where α_{Fe} is the activity of Fe and is equal to $\gamma_{\text{Fe}} N_{\text{Fe}}$ where γ_{Fe} is the activity coefficient and N_{Fe} is the concentration (atomic) of Fe in the solution. ΔS_{Fe} is the change of entropy on melting of Fe which is 7.641 J/Kmol (Robie et al. 1978) at atmospheric pressure and T_{Fe}^m is the melting temperature of pure iron. Textural evidence shows that the eutectic composition contains only a minor amount of FeO; accordingly γ_{Fe} is assumed to be equal to unity. Likewise, within the pressure range employed, it is reasonable to assume that ΔS_{Fe} is approximately independent of pressure. Accordingly, we can calculate the composition of the eutectic point at 16 GPa from (1) using the experimental data $T_{\text{Fe}}^m = 2050^\circ\text{C}$ and $T = 1700^\circ\text{C}$ (Fig. 7). The Fe–FeO eutectic is thereby found to occur at $N_{\text{Fe}} = 0.85 \pm 0.03$. This is in good agreement with our estimate of the eutectic composition based upon textural observations which yielded N_{Fe} between 0.90 and 0.85. Allowance for the effects of a small positive deviation from ideality in the Fe–FeO solution ($\gamma_{\text{Fe}} > 1$) and a small decrease of ΔS_{Fe} with pressure would move the calculated eutectic composition to a slightly higher iron content.

The experimental results depicted in Figure 7 show that a pressure of 16 GPa causes a large increase in the solubility of FeO in molten iron at a given temperature. It follows that the partial molar volume (\bar{V}_{FeO}^m) of FeO dissolved in molten iron (at the eutectic) must be substantially smaller than that of pure wüstite (V_{FeO}^c). The reasons for this behaviour have been discussed in detail by Ringwood (1977, 1984) and Ohtani et al. (1984) and are primarily due to the shorter iron-oxygen bond length in metallic Fe–FeO solutions as compared to the ionic Fe–O bond in wüstite.

Ohtani et al. (1984) showed that it is possible to calculate ΔV , the difference between the partial molar volume of FeO dissolved in iron and the molar volume of pure molten wüstite, from quantitative measurements of the effect of pressure on the solubility of FeO in Fe in the vicinity of the Fe_c –FeO_c eutectic temperature. They obtained a value of $3.8 \text{ cm}^3/\text{mol}$ for ΔV by this technique. Alternative methods (Ohtani et al. 1984) yielded a range of values for ΔV between 2.1 and $3.8 \text{ cm}^3/\text{mol}$. Using an independent

set of measurements of the solubility of FeO in molten iron up to 2500° C (Ohtani and Ringwood 1984; Fischer and Schumacher 1978) together with their preferred ΔV value of 3.8 cm³, they calculated the solubility of liquid FeO in molten iron over a wide range of pressures and temperatures. Their results showed that the liquid immiscibility field contracts dramatically with pressure and disappears at about 20 GPa. Above this pressure the system Fe—FeO contains only a single binary eutectic (analogous to the system Fe—FeS).

We have repeated these calculations using our own data and obtain $\Delta V \geq 2.1$ cm³/mol, which is in satisfactory agreement with the results of Ohtani et al. (1984) considering the various sources of uncertainty. We are able to establish only a lower limit to ΔV because of uncertainty in the position of the eutectic on the FeO-rich side of the phase diagram and the activity of FeO₁. However, because α_{FeO} is necessarily less than unity at the eutectic, the relevant thermodynamic formulations lead to a lower limit to ΔV . Ohtani et al. (1984) did not encounter this uncertainty since under the conditions of their experiments at 3 GPa, the FeO-rich phase in equilibrium with the liquid metallic Fe—FeO solution consisted essentially of stoichiometric liquid FeO, necessarily possessing an activity of unity.

Taking ΔV as 2.1 cm³/mol, existing data on the solubility of FeO in molten iron between 1500–2500° C (Ohtani and Ringwood 1984; Fischer and Schumacher 1978), we have calculated the boundary of the liquid immiscibility field at 16 GPa. This is given by the broken line in Figure 7 which is likely to be an upper limit. The results imply that a pressure of 16 GPa causes a considerable contraction in the extent of the liquid immiscibility field. Whereas at ambient pressure, liquid immiscibility extends to a temperature of about 2800° C (Ohtani and Ringwood 1984), we find that the immiscibility gap closes at about 2200° C at 16 GPa (Fig. 7). Considerable contraction of the liquid immiscibility field at 16 GPa is also required by the experimentally constrained positions of the two eutectics in iron-rich and FeO-rich compositions as shown in Figure 7.

Because of extremely rapid unmixing of liquids during quenching, it is not possible to establish the boundaries of the liquid immiscibility field by the quenching method. It is for this reason that two runs displaying evidence of liquid immiscibility are believed to have actually been carried out in the single phase liquid field (Fig. 7).

6. Miscibility of Molten Iron and Wüstite at 25 GPa

The previous results demonstrate that high pressures cause a considerable increase in the solubility of FeO in molten iron. In order to explore this effect further, a single melting experiment was carried out on the Fe₅₀FeO₅₀ composition at 25 GPa and 2200° C, using 2 mm truncated anvils. The heating duration was 1 min. Photographs of the polished section are shown in Figures 8a, b and c.

The textures show that the entire sample represents a succession of generations of rapidly crystallized wüstite and quenched residual Fe-rich liquids. These textures stand in contrast to those of runs 13-50, 3-50, 17-50 and 15-50 carried out at 16 GPa and equivalent temperatures (1900–2200° C). Throughout most of these latter runs, extensive exsolution of FeO had apparently occurred during quenching, leaving large areas of metallic iron containing little FeO, whilst zones of polygonal FeO crystals were se-

gregated along the inside wall of the MgO capsule. It was only in localised areas which may have experienced relatively rapid quenching, that dense emulsion textures representing liquid-liquid exsolution from a homogeneous precursor were found (e.g. Fig. 6d). It seems that the much more extensive preservation of these quench textures in run 305-50 may reflect faster quenching caused by the smaller cell, possibly combined with lower mobility of FeO caused by the higher pressure.

The microtexture of 305-50 shown in Figure 8a–c displays two distinct domains: (i) Irregularly-shaped FeO-rich domains in which dendritic quenched crystals of FeO occupy about 70 percent of the volume and (ii) Fe-rich domains in which relatively finer FeO dendrites and irregularly-shaped spheroids and blobs are dispersed throughout the metallic matrix. The Fe-rich domains contain 41 ± 3 percent by volume of FeO (23 ± 2 mol % FeO) as determined by point counting on photographs of the polished surface. Inclusion of oxygen dissolved in metallic iron would increase this to 25 ± 2 mole percent FeO. The FeO spheroids sometimes contain inclusions of exsolved iron. The entire sample consists of mixtures of these two domains on varying scales. Electronmicroprobe analyses show that carbon, tungsten and cobalt are below detection limits throughout the interior of the charge. The FeO dendrites in the FeO-rich domains contain about 0.3 percent MgO, whilst the fine FeO dendrites and spheroids in the Fe-rich domains contain much lower concentrations, in the vicinity of 0.05 percent MgO. The metallic iron phase contains up to 0.45 percent O in solid solution or as submicroscopic inclusions of FeO.

The large, irregularly-shaped dendrites of crystalline FeO have evidently crystallized very quickly during quenching, occluding numerous pockets of metallic iron within their interiors. The textures strongly indicate that the run was quenched from above the liquidus and that crystalline FeO was the liquidus phase encountered on decrease of temperature. This implies the existence of complete liquid miscibility between FeO and a composition more iron-rich than Fe₅₀FeO₅₀ under the experimental conditions. The iron-rich regions (25 mol % FeO) can be plausibly interpreted as representing the composition of the Fe—FeO eutectic in the system. A wide variety of rapidly-crystallized quench textures are evident in these regions, including FeO dendrites which precipitated in the crystalline state and spheroids whose origin is more uncertain. The spheroids may indicate a limited region of liquid immiscibility which was encountered in cooling during quenching in an iron-rich composition near the eutectic. However, the shapes of the spheroids are much more irregular than the near-perfect spheres of FeO normally encountered in the stable immiscibility field of the Fe—FeO system (e.g. Ohtani and Ringwood, Fig. 3, 1984). Accordingly, the interpretation of the present spheroidal textures (Fig. 8c) as indicative of liquid immiscibility is not definitive.

If a region of liquid immiscibility does exist at 25 GPa, its extent must be very small. Considering the bulk composition and the amount of crystalline FeO which precipitated, the primary field of crystallization of FeO would extend from FeO₁₀₀ to about Fe₇₅FeO₂₅. Extrapolation of the eutectic composition versus pressure, based on the compositions observed at 0, 4 and 16 GPa indicates that the eutectic at 25 GPa should contain about 20 percent FeO. Thus the composition gap in which immiscibility occurs

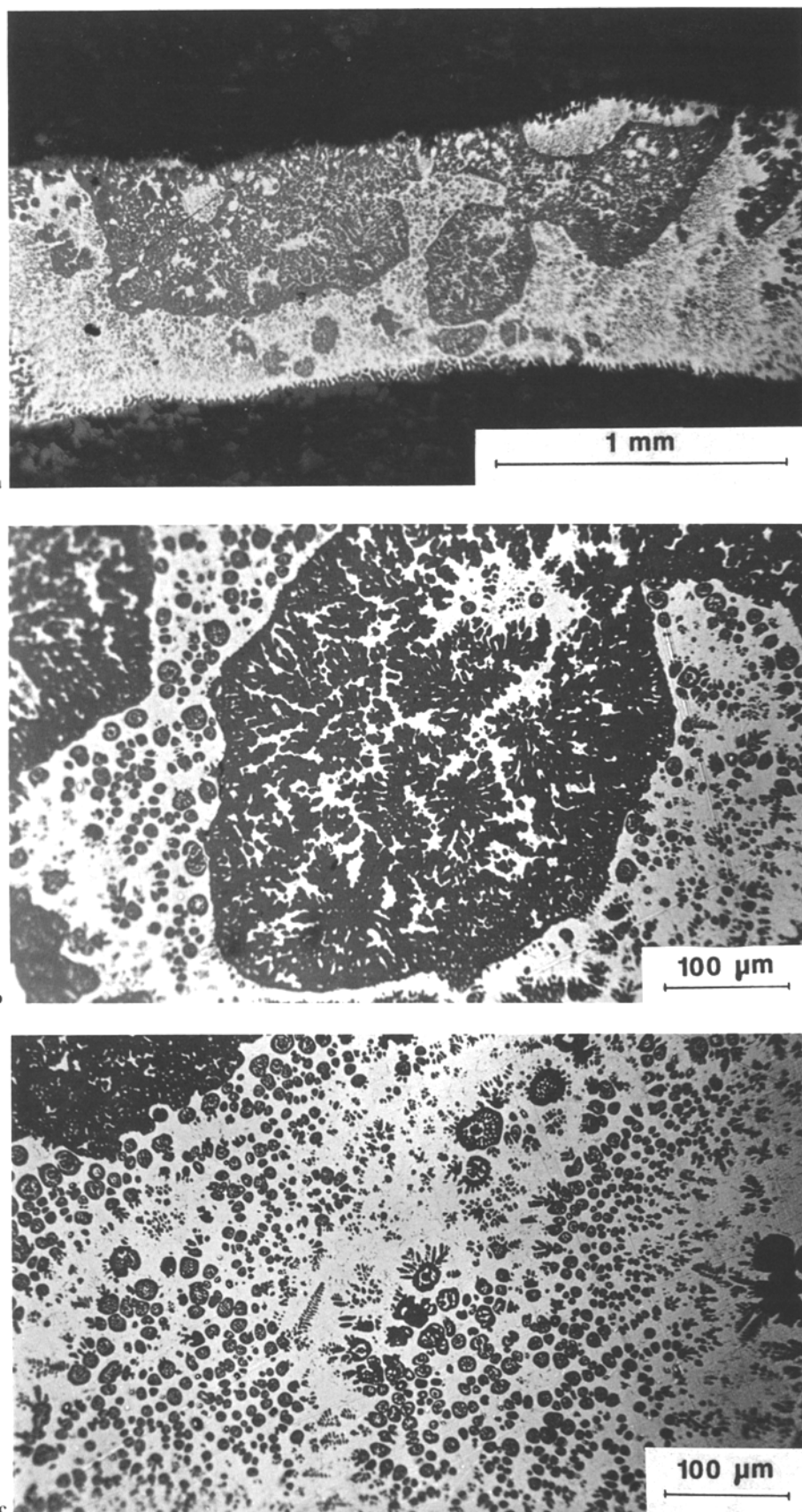


Fig. 8a–c. Polished section of Run 305-50 at 25 GPa and 2200°C. (a) Overall perspective showing contrasting FeO-rich and Fe-rich domains. (b) Detail of FeO-rich domain showing rapid dendrite crystallization of wüstite accompanied by occlusion of iron-rich liquids. (c) Detail of Fe-rich domain showing the wide range of morphologies displayed by wüstite during rapid crystallization

is unlikely to be much larger than the interval $\text{Fe}_{80}\text{FeO}_{20}$ – $\text{Fe}_{75}\text{FeO}_{25}$, if indeed it exists at all. The eutectic temperature at 25 GPa is probably in the vicinity of 1750–1800°C (Fig. 9). Thus, it is unlikely that a small immiscibility gap recurring near the eutectic would extend as high as the run temperature (2200°C). We conclude that complete miscibility between Fe–FeO probably occurs at 2200°C and 25 GPa and that a very small field of liquid immiscibility may possibly be present substantially below this temperature.

7. Composition of the Earth's Core

The results described in sections 4, 5 and 6 above confirm the basic conclusions of Ringwood (1977, 1984), Ohtani and Ringwood (1984) and Ohtani et al. (1984) concerning the effects of high temperatures and pressures on the solubility of FeO in molten iron. Our results are in qualitative agreement with those reported by M. Kato (1985) although our FeO solubilities are somewhat higher than his values. We believe this is because he did not allow adequately for the effects of FeO exsolution during quenching. The significance of this factor was recognised in the subsequent paper by Urakawa et al. (1987).

The implications of these results for the composition of the Earth's core were extensively discussed by Ringwood (1977, 1984), McCammon et al. (1983), Ohtani et al. (1984) and Urakawa et al. (1987). A large part of the core-formation process presumably occurred at much higher pressures and temperatures than those reached in the present experiments. These factors would enhance the solubility of FeO in molten iron. On the other hand, the activity of FeO in lower mantle phases is reduced because of solid solution with MgO, causing a corresponding reduction in FeO solubility. Thermodynamic studies of these effects by the above authors demonstrated that the influence of high P and T on FeO solubility would greatly predominate over the reduction in FeO activity. Accordingly they concluded that if the Earth had formed in a condition whereby metallic iron had been intimately mixed with silicates, as is postulated by the accretion models of Safronov (1978) and others, the subsequent or accompanying segregation of molten iron to form the core would inevitably have been accompanied by the solution of large amounts of FeO in the metallic phase. Thus it was further concluded that oxygen is the principal light element in the Earth's outer core. Shock-wave investigations by Jeanloz and Ahrens (1980) on the density of FeO at high pressures showed that the observed density of the core could be explained if it contained about 40 weight percent of FeO or about 10 weight percent oxygen, in close agreement with an earlier estimate by Ringwood (1977).

Some workers (e.g. Murthy and Hall 1970) have suggested that sulphur is the principal light element in the core, but this proposal encounters some serious difficulties (Ringwood 1984). It implies that the Earth accreted about 30 percent of the primordial abundance of sulphur, which would have been relatively volatile in the solar nebula, whereas many elements which are substantially or considerably less volatile than sulphur (e.g. Na, K, Rb, F, Zn, Cd) were lost from the Earth in proportionally larger amounts. Nevertheless, it seems likely that a small but significant amount of sulphur was accreted by the Earth and entered the core. Ringwood (1977) estimated that the core contains

2–3 weight percent of sulphur, based upon inferred abundances of other volatile elements in the Earth. As will be seen below, this is sufficient to play an important role in the process of core formation.

It is often assumed that the solid inner core is composed essentially of pure nickel-iron but this seems doubtful. Light elements normally form a wide range of metallic or semimetallic compounds with iron, e.g. Fe_3C , Fe_2C , Fe_4N , Fe_2N , Fe_2B , Fe_3Si , FeSi , FeS . Crystalline wüstite is known to transform to the metallic state at 70 GPa (Knittle and Jeanloz 1986) and at the much higher pressures pertaining in the inner core, the possibility of formation of additional stable metallic phases such as Fe_2O , Fe_3O , Ni_2O , Ni_3O and their solid solutions must be seriously considered. It seems quite possible that the inner core consists of an $(\text{Fe}, \text{Ni})_2\text{O}$ phase (Dubrovskiy and Pan'kov 1972; Ringwood 1984). This interpretation is consistent with the conclusion of Jephcoat and Olsen (1987) that the density of the inner core is significantly smaller than that of pure iron and that this region therefore contains a significant amount of a light element(s).

8. Temperature Regime and Core Formation

Williams et al. (1987) concluded that the temperature at the boundary of the outer and inner core is 7000–8000°C, assuming that the inner core is composed of pure iron. This would imply a temperature of at least 5000°C at the boundary between the outer core and mantle. On the other hand, Heinz and Jeanloz (1987) concluded that the melting temperature of MgSiO_3 perovskite near the base of the lower mantle is only about 3000°C. It is very difficult to reconcile these greatly contrasting temperatures, even if it is assumed that a substantial thermal boundary layer is present at the base of the mantle. Moreover, a temperature of 7000–8000°C at the inner core boundary would imply that the Earth was formed in a completely molten state. Recent studies of mantle differentiation (Kato et al. 1988a) do not support this implication.

These dilemmas might be avoided by considering the thermal effects of light elements in the core. If the inner core consists of $(\text{Fe}, \text{Ni})_2\text{O}$, its melting temperature could be substantially smaller than that of pure iron. Both the melting point and the melting point gradient of iron are lowered considerably by the presence of light elements. It is seen from Figure 9 that the temperature gradient of the Fe–FeO eutectic is much smaller than that of pure iron. This low gradient is expected to persist at least to 70 GPa where FeO transforms to the metallic state (Knittle and Jeanloz 1986). The results of Urakawa et al. (1986) show that both the melting point and the gradient of the FeO–FeS–Fe cotectic are dramatically lower than those of pure iron (Fig. 9) and are lowered still further by the presence of nickel. Recently, Kato et al. (1988b) showed experimentally that the mantle solidus at 25 GPa is higher than 2200°C. The results described in Section 6 show that Fe and FeO would form a liquid solution at a substantially lower temperature than this¹. The liquidus temperature would be reduced still further by the presence of significant amounts of sulphur and nickel (Fig. 9). Accordingly, it

¹ Note that the experiments on the mantle silicate and Fe–FeO systems were carried out using the same experimental techniques so that this comparison is independent of ambiguities arising from inter-laboratory calibrations of pressure and temperature

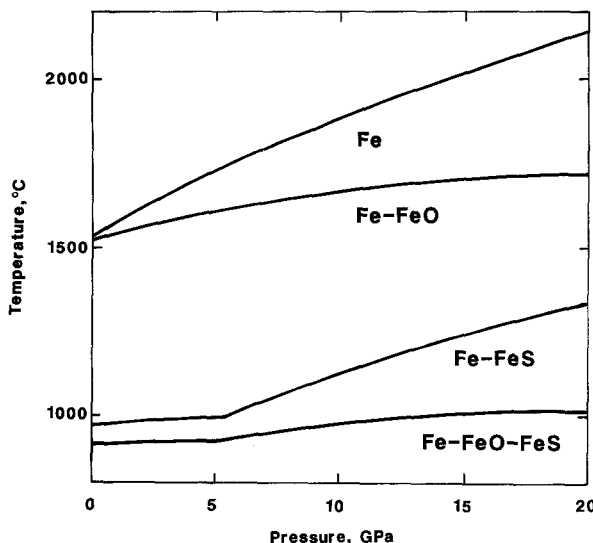


Fig. 9. Variations of melting temperatures with pressure for Fe, the Fe-FeO and Fe-FeS eutectics, and the Fe-FeO-FeS co-tectic. Data for Fe from Boehler (1986), Fe-FeO (Ohtani et al. 1984 and this study), Fe-FeS (Usselman 1985) and Fe-FeO-FeS from Urakawa et al. (1987).

seems likely that the melting point of an alloy containing, say, 84% Fe, 6% Ni, 7% O and 3% S by weight would be below the mantle solidus at all depths, thereby removing the difficulties noted above.

Formation of the core via segregation of a metallic Fe-Ni-O-S liquid within the Earth has recently been discussed by Urakawa et al. (1987). Core-segregation probably occurred contemporaneously with accretion. After the Earth had grown to a critical size, heating of the outer layers via partial retention of gravitational accretional energy would have caused partial melting of the Fe-Ni-O-S phase. The first liquid to form would have been rich in sulphur. As it sank through the mantle, increasing amounts of oxygen would have dissolved in the melt. Gravitational energy released by segregation of metal into the core raised the internal temperature within the Earth, thereby increasing the solubility of oxygen in the metal and the degree of melting of metal phase. Ultimately all of the metal phase would have been melted, followed by its segregation into the core.

Urakawa et al. (1987) showed that at high pressures, the Fe-Ni-O-S liquid readily wets the surfaces of silicate crystals and migrates through the silicate grain boundaries. This would cause a close approach to local chemical equilibrium between metal and silicates. The liquid metal would then segregate into bodies which were large enough to sink through the surrounding silicates into the core (Elssasser 1963). The rate of sinking of these larger bodies may have been too rapid to permit chemical equilibrium to have been maintained (Ringwood 1959; Stevenson 1981). Thus, the core would have formed by the mixing of batches of liquid which had equilibrated locally with surrounding mantle silicates over a very wide range of pressures and temperatures. The distributions of siderophile elements between metal and silicate may therefore have varied widely, according to the local P, T conditions which prevailed. If the core formed in this manner, it would be out of chemical equilibrium with the mantle at the essentially fixed P and T conditions defined by the core-mantle boundary. Chemi-

cal reactions and transport of elements may therefore occur across this boundary, possibly accounting for some of the anomalous seismic properties of the D'mantle layer immediately adjacent to the core (Ringwood 1959; Stevenson 1981).

Acknowledgements. The authors are indebted to Mr. N. Ware for assistance with the electroprobe analyses and to Dr. D. Ellis and Dr. S. Kesson of the ANU for helpful comments on the manuscript.

References

- Birch F (1964) Density and composition of mantle and core. *J Geophys Res* 69:4377-4388
- Boehler R (1986) The phase diagram of iron to 430 kbar. *Geophys Res Lett* 13:1153-1156
- Dubrovskiy VA, Pan'kov V (1972) On the composition of the earth's core *Izv. Phys Solid Earth* 7:48-54
- Elssasser WM (1963) Early history of the earth. In: Geiss J, Goldberg E (eds) *Earth science and meteorites*, North Holland, Amsterdam, pp 1-30
- Fischer WA, Schumacher JF (1978) Die Sättigungslöslichkeit von Reineisen an Sauerstoff vom Schmelzpunkt bis 2046°C, ermittelt mit dem Schwelbeschmelzverfahren. *Arch Eisenhüttenwes* 49:431-435
- Getting IC, Kennedy GC (1970) Effect of pressure on the e.m.f. of chromel-alumel and platinum-platinum, 10% rhodium thermocouples. *J Appl Phys* 41:4552-4562
- Hansen M, Anderko K (1958) *Constitution of binary alloys*. McGraw Hill, New York
- Heinz DL, Jeanloz R (1987) Measurement of the melting curve of $Mg_{0.9}Fe_{0.1}SiO_3$ at lower mantle conditions and its geophysical implications. *J Geophys Res* 92:11437-11444
- Irifune T, Hibberson WO (1985) Improved furnace design for multiple anvil apparatus for pressures up to 18 GPa and temperatures to 2000°C. *High Temp High Press* 17:575-579
- Jeanloz R, Ahrens T (1980) Equation of state of FeO and CaO. *Geophys JR Astron Soc* 62:505-528
- Jephcoat AP, Olson P (1987) Is the inner core of the earth pure iron? *Nature* 325:332-335
- Kato M (1985) Melting experiment on Fe-FeO-FeS system up to 20 GPa and its significance on the formation and composition of the earth's core. PhD Thesis, Nagoya University
- Kato T, Kumazawa M (1985) Effect of high pressure on the melting relation in the system Mg_2SiO_4 : Part I Eutectic relation up to 7 GPa. *J Phys Earth* 33:513-524
- Kato T, Kumazawa M (1986) Melting and phase relations in the system Mg_2SiO_4 -MgSiO₃ at 20 GPa under hydrous conditions. *J Geophys Res* 91:9351-9355
- Kato T, Ringwood AE, Irifune T (1988a) Experimental determination of element partitioning between silicate perovskites, garnets and liquids: Constraints on early differentiation of the mantle. *Earth Planet Sci Lett* 89:123-145
- Kato T, Ringwood AE, Irifune T (1988b) Constraints on element partition coefficients between MgSiO₃ perovskite and liquid determined by direct measurements. *Earth Planet Sci Lett* 90:65-68
- Knittle E, Jeanloz R (1986) High pressure metallization of FeO and implications for the Earth's core. *Geophys Res Lett* 8:1541-1544
- Lindsley DH (1966) Pressure-temperature relations in the system FeO-SiO₂. *Ann Rept Geophys Lab* 65:226-230
- Liu LG, Bassett WA (1975) The melting of iron up to 200 kb. *J Geophys Res* 80:3777-3782
- McCammon CA, Ringwood AE, Jackson I (1983) Thermodynamics of the system Fe-FeO-MgO at high pressure and temperature and a model for formation of the Earth's core. *Geophys J R Astron Soc* 72:577-595
- Murthy VR, Hall H (1970) The chemical composition of the

- Earth's core: Possibility of sulfur in the core. *Phys Earth Planet Inter* 2:276–282
- Ohtani E, Ringwood AE (1984) Composition of the core, I. Solubility of oxygen in molten iron at high temperatures. *Earth Planet Sci Lett* 71:85–93
- Ohtani E, Ringwood AE, Hibberson WO (1984) Composition of the core, II. Effect of high pressure on solubility of FeO in molten iron. *Earth Planet Sci Lett* 71:94–103
- Ohtani E, Ringwood AE, Major A, Hibberson WO (1984) Solubilities of NiO and CoO in molten nickel and cobalt. (Unpublished experimental results and manuscript)
- Ohtani E, Irifune T, Ringwood AE, Hibberson WO (1987) Modified split-sphere guideblock for practical operation of a multiple-anvil. *High Temp High Press* 19:523–529
- Ringwood AE (1959) On the chemical evolution and densities of the planets. *Geochim Cosmochim Acta* 15:257–283
- Ringwood AE (1977) Composition of the core and implications for the origin of the earth. *Geochem J* 11:111–135
- Ringwood AE (1984) The Earth's core: its composition, formation and bearing upon the origin of the Earth. *Proc R Soc London A* 395:1–46
- Ringwood AE, Major A (1982) Mutual solubilities of molten transition metals and oxides. *Lunar Planet Sci XIII Part 2*:651–652
- Safronov VS (1978) Evolution of the protoplanetary cloud and formation of the Earth and planets, Translated from the Russian, Israel Program for Scientific Translations. Tel Aviv
- Sterrett KF, Clement W, Kennedy GC (1965) Effect of pressure on the melting of iron. *J Geophys Res* 70:1979–1984
- Stevenson DJ (1981) Models of the earth's core. *Science* 214:611–619
- Tankens ES, Gokcen NA, Belton GR (1964) The activity and solubility of oxygen in liquid iron, nickel and cobalt. *Trans Metallurgical Soc AIME* 230:820–827
- Urakawa S, Kato M, Kumazawa (1987) Experimental study on the phase relations in the system Fe–Ni–O–S up to 15 GPa. In: Manghnani MH, Syono Y (eds) High-Pressure Research in Mineral Physics. Terra Scientific Publishing Company Tokyo, pp 95–111
- Usselman TM (1975) Experimental approach to the state of the core: Part 1. The liquidus relations of the Fe-rich portion of the Fe–Ni–S System from 30 to 100 kb. *Am J Sci* 275:278–290
- Williams Q, Jeanloz R, Bass J, Svendsen B, Ahrens T (1987) The melting curve of iron to 250 GPa: constraint on the temperature at the Earth's center. *Science* 236:181–182
- Wood BJ, Fraser DG (1977) Elementary thermodynamics for geologists. Oxford University Press, Oxford

Received October 25, 1988